AA 529 HW4

Matt Russell
https://github.com/russellmatt66/aa529-hw/tree/main/hw4

June 5, 2021

Contents

1 Introduction

The script *main_aa529hw4.py* found at the repo listed in the title page does the computations necessary to solve most of the assignment.

2 Problem 1

$$I_{sp} = 1200 \quad [s] \tag{1}$$
$$\eta_T = 0.6 \tag{2}$$
$$m_i = m_{Xe} = 131 \quad [amu] \tag{3}$$
$$g_0 = 9.819 \quad [m(s)^{-2}] \tag{4}$$

Starting with the thrust efficiency of an ion thruster,

$$\eta_T = \frac{KE_{ion}}{KE_{ion} + \epsilon_{cost}} \tag{5}$$

can be rearranged,

$$\epsilon_{cost} = KE_{ion}\frac{(1-\eta_T)}{\eta_T} \tag{6}$$

and the kinetic energy of an ion written in terms of the specific impulse of the propulsion process,

$$KE_{ion} = \frac{m_i}{2}(g_0 I_{sp})^2 \tag{7}$$

The result of this computation for a Xenon ion thruster is an energy cost per ion of,

$$\epsilon_{cost} = 63.162 \quad [eV/ion] \tag{8}$$

which illustrates the low efficiency that this kind of thruster will suffer from when the device is operating at an intermediate level of I_{sp}. Electrothermal thrusters suffer from this same problem which creates a space for a new, presently un-developed, propulsion technology.

3 Problem 2

An Argon MPDT has the following characteristics,

$$r_c = 0.02 \quad [m] \tag{9}$$
$$r_a = 0.07 \quad [m] \tag{10}$$
$$J = 20 \quad [kA] \tag{11}$$

3.1 (a)

The thrust coefficient of the propulsion device is,

$$C_T = \frac{4\pi}{\mu_0} \frac{T}{J^2} \tag{12}$$

The thrust on the body, T, which is considered here to arise from an axial 'blowing' and radial 'pumping' due to electromagnetic body forces on the flow is given by the Maeker equation,

$$T = \frac{mu_0 J^2}{4\pi} \left(ln(\frac{r_a}{r_c} + \frac{3}{4} \right) \tag{13}$$

which gives,

$$C_T = 2.003 \tag{14}$$

3.2 (b)

In the discharge region the field strength varies in the radial direction in a piecewise manner. A plot illustrating this is shown in Fig 1 The maximum field strength of $B = 0.2$ [T] occurs at a radial position of

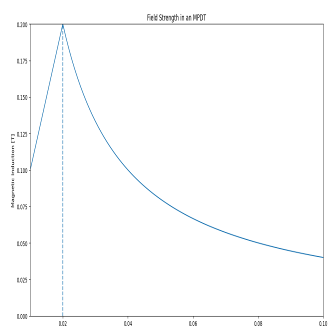

Figure 1: Once outside the region where a current density is flowing the B-field falls off with a $\frac{1}{r}$ dependence due to Ampere's Law.

$r = 0.02$ [m], which corresponds to the cathode edge.

3.3 (c)

The balance of forces between the electromagnetic (Lorentz) body-forces and the pressure gradient in the device,

$$\vec{J} \times \vec{B} = \boldsymbol{\nabla} p \tag{15}$$

defines the equilibrium. The radial distribution of pressure can be solved for by assuming an azimuthal magnetic field which is generally not true downstream from the cathode,

$$p(r) = p_0 + \frac{\mu_0 J^2}{4\pi^2 r_c^2} \left(1 - (\frac{r}{r_c})^2 \right) \tag{16}$$

The greatest differential occurs at the centerline of the cylindrically-symmetric nozzle, $r = 0$,

$$p - p_0|_{greatest} = 0.314 \quad [atm] \tag{17}$$

which is illustrated in Figure 2

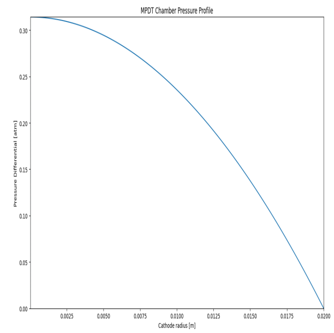

Figure 2: The high pressure near the cathode tip can lead to fatigue and erosion, the latter of which is typically the dominant life-limiting factor in electric propulsion devices

3.4 (d)

The axial, 'blowing', force is calculated by integrating the Lorentz force density over the discharge volume,

$$F_z = \frac{\mu_0 J^2}{4\pi} \left[ln(\frac{r_a}{r_c} + \frac{1}{4} \right] \tag{18}$$

$$F_z = 90.111 \quad [N] \tag{19}$$

3.5 (e)

The radial, 'pumping', force is calculated in a similar way as for the axial force,

$$F_c = \frac{\mu_0 J^2}{8\pi} \tag{20}$$

$$F_c = 20 \quad [N] \tag{21}$$

3.6 (f)

The thrust is taken to be the sum of the two force contributions,

$$T = F_z + F_c \tag{22}$$

$$T = 110.111 \quad [N] \tag{23}$$

4 Problem 3

Besides the values given in the problem statement, the following are assumed:

$$\dot{x} = 5.0 \times 10^4 \quad [m/s] \tag{24}$$

$$x(0) = 0 \tag{25}$$

4.1 (a)

The alpha's for each thruster,

$$\alpha_A = 2.84 \times 10^{-4} \tag{26}$$

$$\alpha_B = 1.8 \times 10^{-5} \tag{27}$$

$$\alpha_C = 9.7 \times 10^{-5} \tag{28}$$

and the beta's,

$$\beta_A = 0.316 \tag{29}$$

$$\beta_B = 0.316 \tag{30}$$

$$\beta_C = 1.739 \tag{31}$$

4.2 (b)

Thruster A and B are critically-damped: $\beta_{A,B} = 0.316 \sim 1$ and are represented by the Green curve. Thruster C is also critically-damped: $\beta_C = 1.739 \sim 1$ and represented by the same curve as A and B are. Blue and Orange show oscillations characteristic of an underdamped system, which are not represented among the thrusters. None of the curves are shaped like an over-damped system, which would appear superficially similar to the critically-damped, Green example curve but with a shorter peak and much broader width, i.e fall-time.

4.3 (c)

The ratio, $\frac{\Delta L_p}{L_0}$, for each thruster is,

$$ratio_A = 5.027 \tag{32}$$

$$ratio_B = 1.257 \tag{33}$$

$$ratio_C = 1.257 \tag{34}$$

which implies that they all satisfy the Lovberg criteria. This criterion is particularly important to a pulsed plasma thruster (PPT) as it gives a theoretical upper bound on the electrical efficiency of the acceleration process. Naturally, η_e cannot go above 1 so care must be taken in interpreting the number. Extreme values, i.e, far from 1, would indicate excessive resistive lossess (small ΔL) or a decoupling of the plasma current layer from the accelerator mechanism (large ΔL).

4.4 (d)

Thruster B is the most efficient thruster. A look at the Lovberg parameter indicates that A's operation is experiencing a large change in the total inductance relative to the circuit inductance which can be explained by the slug experiencing partial decoupling from the accelerator rails during the acceleration process. For a linear one this value is given by,

$$\Delta L_p = \mu_0 \frac{h}{d} l \tag{35}$$

indicating that the channel aspect ratio of A is the limiting factor here. An increase to the height of the channel would correspond to a greater proclivity on the part of the plasma to kink, or suffer from dynamic

instability. Because plasma is a conductive medium the disconnection or formation of alternate current-carrying branches due to deformation of the slug would end up reducing the flux of charged particles in the system and negatively impact the performance of the overall process as a result, either by reducing the kinetic energy in the exhaust gas or through introducing a global decoherence in the entire structure.
Thruster C has the same Lovberg parameter has Thruster B so it is fair to assume from this that both are operating in similar capacities. However, Thruster C can be argued to suffer from greater resistive losses than B due to its higher Voltage and Circuit Resistance.

5 Problem 4

The specific impulse can be estimated from,

$$I_{sp} = \frac{2\eta_T}{g_0}\frac{P}{T} \tag{36}$$

$$= 63.783 \quad [sec] \tag{37}$$

where a thrust efficiency, $\eta_T = 0.65$ was chosen. The thrust-to-power ratio of the maiden resistojet satellite was obtained from Chapter 6 of Jahn[1].

Note that a naive analysis might try and estimate the above from a calculation of the exhaust velocity based on an assumption of adiabatic nozzle flow; however, by nature the expansion process in a resistojet is non-adiabatic so this sequence of computations will lead to misleading results.

From an engineering perspective one of the advantages of using an N_2 monopropellant for a resistojet is that the fuel is already in gaseous form. However, from a cost and logistical perspective its high molecular weight is a disadvantage as the increased bulk resists being transported.

References

[1] Robert G Jahn. *Physics of electric propulsion*. New York, 1968.